THE JOURNAL OF PHYSICAL CHEMISTRY A

 VOLUME 112, NUMBER 13, APRIL 3, 2008

ARTICLES

Ultrafast Intramolecular Charge Transfer with Strongly Twisted Aminobenzonitriles: 4-(Di-*tert*-butylamino)benzonitrile and 3-(Di-*tert*-butylamino)benzonitrile

Sergey I. Druzhinin,[†] Srinivas Reddy Dubbaka,[‡] Paul Knochel,*[,‡] Sergey A. Kovalenko,*[,§] Peter Mayer,[‡] Tamara Senyushkina,[†,§] and Klaas A. Zachariasse*[,†]

Max-Planck-Institut für biophysikalische Chemie, Spektroskopie und Photochemische Kinetik, 37070 Göttingen, Germany, Department Chemie und Biochemie, Ludwig-Maximilians-Universität, Butenandtstrasse 5-13, Haus F, 81377 München, Germany, and Institut für Chemie, Humboldt Universität zu Berlin, Brook-Taylor Strasse 2, 12489 Berlin, Germany

Received: October 5, 2007; In Final Form: December 18, 2007

The newly synthesized aminobenzonitriles with two bulky amino substituents 4-(di-*tert*-butylamino)benzonitrile (DTABN) and 3-(di-*tert*-butylamino)benzonitrile (mDTABN) have strongly twisted amino groups in the ground state. From X-ray crystal analysis it is found that the amino twist angle θ of mDTABN equals 86.5°, whereas a twist angle of around 75° is deduced for DTABN from the extinction coefficient of its lowest-energy absorption band in *n*-hexane. Because of the electronic decoupling between the amino and benzonitrile groups caused by these large twist angles, the absorption of DTABN and mDTABN is relatively weak below 40000 cm^{-1}, with extinction coefficients around 25 times smaller than those of the planar 4-(dimethylamino)-benzonitrile (DMABN). DTABN as well as mDTABN undergo efficient intramolecular charge transfer (ICT) in the singlet excited state, in nonpolar (*n*-hexane) as well as in polar (acetonitrile) solvents. Their fluorescence spectra consist of an ICT emission band, without evidence for locally excited (LE) fluorescence. The occurrence of efficient ICT with mDTABN is different from the findings with all other *N,N*-dialkylaminobenzonitriles in the literature, for which ICT only appears with the para-derivative. From solvatochromic measurements, an ICT dipole moment of 17 D is determined for DTABN as well as for mDTABN, similar to that of DMABN. The picosecond fluorescence decays of DTABN (time resolution 3 ps) are effectively single exponential. Their decay time is equal to the ICT lifetime τ'_0(ICT), which increases with solvent polarity from 0.86 ns in *n*-hexane to 3.48 ns in MeCN at 25 °C. The femtosecond excited-state absorption (ESA) spectra of DTABN in *n*-hexane and MeCN at 22 °C show a decay of the LE and a corresponding rise of the ICT absorption. The ICT reaction time is 70 fs in *n*-hexane and 60 fs in MeCN. DTABN and mDTABN may have a strongly twisted ICT state, similar to that of 6-cyanobenzoquinuclidine but different from that of DMABN.

Introduction

Intramolecular charge transfer (ICT) with 4-(dimethylamino)-benzonitrile (DMABN) in the singlet excited-state has been extensively studied since its discovery in 1959.[1−21] With DMABN, ICT and dual fluorescence from a locally excited (LE) state and an ICT state is observed in a variety of solvents, from the weakly polar dialkyl ethers and toluene to the strongly polar alkyl cyanides and alcohols.[1−10] ICT emission is, however, practically absent for DMABN in alkane solvents,[4,11−14] and it is not detected at all in crystals,[15] supersonic jets,[16−18] and the vapor[13,18] phase.

Upon increasing the alkyl chain length in the 4-(dialkylamino)benzonitriles, from methyl to *n*-pentyl and *n*-decyl, ICT fluorescence starts to appear in alkane solvents such as cyclohexane.[7,11,12,18−21] The ICT/LE fluorescence quantum yield

* Corresponding authors. Fax: +49-551-201−1501. E-mail: (P.K.) knoch@cup.uni-muenchen.de; (S.A.K.) skovale@chemie.hu-berlin.de; (K.A.Z.) kzachar@gwdg.de.

[†] Max-Planck-Institut für biophysikalische Chemie, Spektroskopie und Photochemische Kinetik.

[‡] Department Chemie und Biochemie, Ludwig-Maximilians-Universität.

[§] Institut für Chemie, Humboldt Universität zu Berlin.

10.1021/jp7097526 CCC: $40.75
Published on Web 03/11/2008

CHART 1

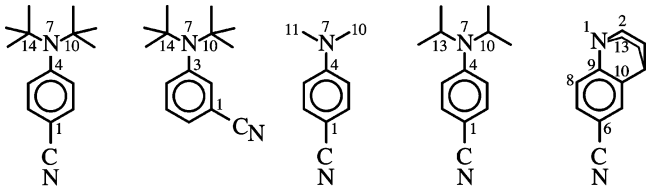

ratio Φ'(ICT)/Φ(LE) in cyclohexane at 25 °C increases in the series DMABN, 4-(diethylamino)benzonitrile (DEABN), 4-(di-*n*-propylamino)benzonitrile (DPrABN) and 4-(di-*n*-decylamino)-benzonitrile (DDABN) as follows: 0.01 (DMABN), 0.16 (DEABN), 0.28 (DPrABN), 0.42 (DDABN).[11] A similar influence of the alkyl chain length occurs for the 4-(dialkylamino)-benzonitriles in toluene.[20]

A much larger increase in ICT efficiency is observed by replacing the *n*-alkyl groups by an isopropyl substituent. With 4-(diisopropylamino)benzonitrile, (DIABN) a fast ICT reaction (3 ps) is found in *n*-hexane at 25 °C.[22] Efficient ICT also takes place with DIABN in the crystal and even in the gas phase.[18,23] The larger ICT efficiency of DIABN has been attributed to its relatively small energy gap $\Delta E(S_1,S_2)$ between the two lowest excited singlet states.[22]

Similar to the influence of the isopropyl groups in DIABN, also the replacement of one of the methyl groups of DMABN by a *tert*-butyl substituent, giving 4-(*tert*-butyl-methylamino)-benzonitrile (tBMABN), leads to a strong enhancement of the ICT efficiency with this compound in *n*-hexane (Φ'(ICT)/Φ(LE) = 25 in *n*-hexane at 25 °C),[24] whereas ICT is absent with DMABN in this solvent, as mentioned above.[24]

With 1-methyl-6-cyano-1,2,3,4-tetrahydroquinoline (NMC6), an ICT reaction does not take place.[3,6,20,24−26] In the case of 1-isopropyl-6-cyano-1,2,3,4-tetrahydroquinoline (NIC6) the presence of the isopropyl substituent now does not lead to ICT.[24] Only with 1-*tert*-butyl-6-cyano-1,2,3,4-tetrahydroquinoline (NTC6) is fast and efficient ICT observed in *n*-hexane and even in the gas phase,[24,25] showing that for obtaining ICT with *N*-alkyl tetrahydroquinolines a *tert*-butyl substituent is more effective than isopropyl. For the molecules tBMABN and NTC6, the increase in ICT efficiency as compared with that of DMABN and NMC6 is caused by a decrease of the energy gap $\Delta E(S_1,S_2)$.

It was therefore considered to be of interest to synthesize 4-(di-*tert*-butylamino)benzonitrile (DTABN, Chart 1). In the first attempts of this synthesis, from 4-aminobenzonitrile (ABN) and *tert*-butyl iodide or as an alternative from 4-fluorobenzonitrile with di(*tert*-butyl)amine, only 4-(*tert*-butylamino)benzonitrile (TABN) was obtained. By employing a new procedure described here, a successful synthesis of DTABN was achieved. Also 3-(di-*tert*-butylamino)benzonitrile (mDTABN) was synthesized.

The synthesis of mDTABN was attempted, although until now ICT has not been observed with *m*-aminobenzonitriles,[27−35] such as 3-aminobenzonitrile (mABN),[11,27,28,33,34] 3-(methylamino)benzonitrile (mMABN),[28] 3-(dimethylamino)benzonitrile (mDMABN),[27−32,35] and 3-(diethylamino)benzonitrile[11,28] (mDEABN). Similarly, ICT could not be found with the *o*-aminobenzonitriles 2-aminobenzonitrile (oABN)[33,34] and 2-(dimethylamino)benzonitrile[30,35,36] (oDMABN). Within the context of the TICT hypothesis, with perpendicular and hence decoupled dimethylamino groups, ICT would be expected to occur with all three dimethylaminobenzonitriles DMABN, mDMABN, and o-DMABN, contrary to observation. Negative effects on the ICT energetics of mDMABN and oDMABN, such as differences in the energy of the LE state, lower for mDMABN and oDMABN than for DMABN,[27−34] and in the formal Coulomb energies of the TICT states of these molecules could easily be overcome due to the large stabilization energy of the ICT state when going from *n*-hexane to MeCN, which amounts to ∼0.8 eV for DMABN.[5,12,31]

SCHEME 1. Synthesis Procedure of 4-(Di-*tert*-butylamino)benzonitrile (DTABN)

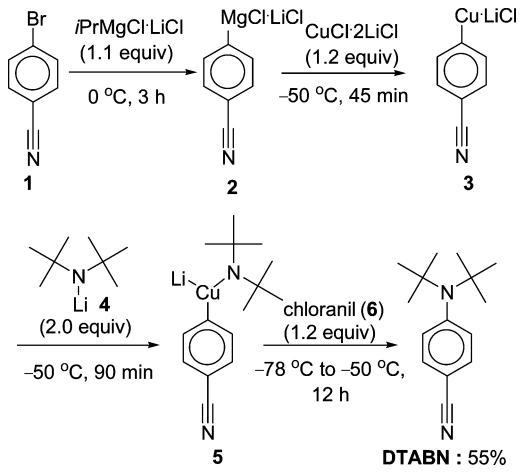

In this paper, the photophysics of DTABN and mDTABN is presented. The amino group of both molecules is strongly twisted in the ground state, as deduced from the crystal structure of mDTABN and from the strongly reduced extinction coefficient of the lowest-energy absorption band of DTABN. Photostationary and time-resolved fluorescence measurements are reported and, in the case of DTABN, femtosecond excited-state absorption spectra are discussed.

Experimental Section

Synthesis of DTABN and mDTABN. Yamamoto[37] and Ricci[38] reported an oxidative coupling of amidocuprates with oxygen, leading to amines. Recently,[39] a new general amination procedure was developed using the readily available polyfunctional lithium amidocuprates. The scope of this method is quite broad with a high functional group tolerance, and it is not hampered by steric hindrance. This procedure employing lithium amidocuprates was used here for the synthesis of DTABN (Scheme 1). Neat 4-bromobenzonitrile **1** was added to *i*PrMgCl·LiCl[40] (1.1 equiv, 0 °C, 3 h), leading to the arylmagnesium derivative **2**. Subsequently, CuCl·2LiCl (1.2 equiv) was added dropwise under argon at −50 °C and the mixture was stirred for 45 min to form copper derivative **3**. Addition of *N*-lithium di-*tert*-butylamide 4 (2 equiv, −50 °C, 90 min), followed by that of chloranil (**6**, 1.2 equiv, −78 to −50 °C, 12 h), resulting in the formation of DTABN with a yield of 55%. As DTABN is acid sensitive, the purification was carried out by chromotography using silica deactivated with triethylamine (2%).

Details of the synthesis procedure for DTABN and mDTABN can be found in the Supporting Information. For the present investigations, DTABN and mDTABN were purified by column chromatography over Al_2O_3, as well as in some cases by HPLC as the last purification step. These compounds proved to be less stable than other aminobenzonitriles (DMABN, DIABN, NTC6) investigated previously, which made their purification more difficult.[8,22,24]

Photostationary and Time-Resolved Measurements. The compounds 4-methylbenzonitrile (4MBN, Aldrich) and 6-cyanobenzoquinuclidine (CBQ)[19] were purified by HPLC. The solvents were chromatographed over Al_2O_3 just prior to use. The solutions, with an optical density between 0.4 and 0.6 for the maximum of the first band in the absorption spectrum, were deaerated by bubbling with nitrogen for 15 min. The measurement of the absorption and fluorescence spectra and the

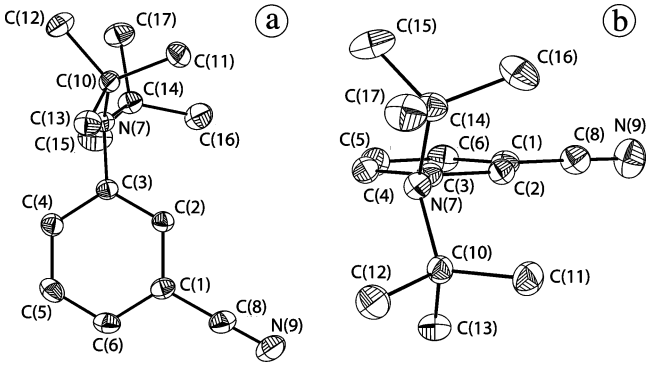

Figure 1. ORTEP diagrams of 3-(di-*tert*-butylamino)benzonitrile (mDTABN), with a view (a) from above and (b) along the axis from the amino nitrogen to the cyano group.

fluorescence quantum yields was described earlier.[8] The fluorescence decay times were determined with a picosecond laser (λ_{exc}: 272 nm) single-photon counting (SPC) system,[41,42] two time ranges being routinely measured simultaneously (0.5 and 10 ps/channel in up to 1800 effective channels). The estimated reproducibility is better than 10% for the ps decay times. The femtosecond transient absorption setup has been described in detail elsewhere.[43,44] DTABN in *n*-hexane or acetonitrile at room temperature (22 °C) was excited with 1 μJ, 70 fs pulses at 327 nm. The pump-induced transient absorption signal was monitored with a supercontinuum probe in the range 272−692 nm.[8]

Crystal Structure Determination and Refinement. A crystal suitable for X-ray crystallography was selected by means of a polarizing microscope, mounted on the tip of a glass fiber, and measured at 200 K on a Nonius KappaCCD diffractometer using Mo Kα radiation (graded multilayer X-ray optics). The structure was solved by direct methods with SIR97[45] and refined by full-matrix least-squares calculations on F^2 with SHELXL-97.[46] Anisotropic displacement parameters were refined for all non-hydrogen atoms. The hydrogen atoms were calculated in idealized geometry riding on their parent atoms. Crystallographic data for mDTABN have been deposited with the Cambridge Crystallographic Data Centre (CCDC No. ost 658250).

Results and Discussion

Crystal Structure of mDTABN. The molecular structure of mDTABN (Figure 1) was determined by X-ray crystal analysis. The experimental data for the bond lengths, bond angles, amino twist angle θ and pyramidal angle φ of this molecule are collected in Table 1. For comparison, crystal data for NTC6,[47] 3,5-dimethyl-4-(dimethylamino)benzonitrile (MMD)[48] and DMABN[48] are also listed. The crystal structure of DTABN could not be analyzed with confidence, as the correct space group of the crystal could not yet be established.

The most striking property of the mDTABN structure (Figure 1) is the nearly perpendicular di(*tert*-butyl)amino group, with a twist angle θ of 86.5° with respect to the plane of the phenyl ring (Table 1). A further structural difference between mDTABN and the other aminobenzonitriles in Table 1 and Figure 2 involves the bond length between the amino nitrogen and the benzonitrile moiety. This crystal amino-phenyl bond length in the series of compounds DMABN, DIABN,[22,49,50] NTC6, MMD, mDTABN, and CBQ[50] becomes longer with increasing amino twist angle θ (Figure 2 and Table 1), from 136.5 pm for DMABN (θ = 2.2°), 137.2 pm for DIABN (θ = 14.3°), and 141.1 pm for MMD (θ = 57°) to 143.7 pm for mDTABN (θ = 86.5°) and 144.7 pm for CBQ (θ = 88.7°). For the last two molecules, the bond length approaches that of a single C−N bond (147 pm), as in methylamine.[51] With DMABN, the N(7)−C(4) bond length is in between that of a single C−N and a double C═N bond (128 pm, as in oximes and imines).[51]

Another difference is in the N(7)−C(10) amino−alkyl bond length, which for mDTABN (150.4 pm) is much longer than for MMD (144.1 pm) and DMABN (144.8 pm). A similar bond lengthening caused by steric hindrance has been observed with NTC6 (149.3 pm, Table 1).[25] Furthermore, the pyramidal angle φ (32.4°) of the amino nitrogen of mDTABN is larger than that of MMD (24.4°), NTC6 (9.6°), and DMABN (8.6°). This angle is related to the sum ΣN of the angles around the amino nitrogen, decreasing when φ becomes larger (Table 1).

Absorption and Fluorescence Spectra of DTABN in *n*-Hexane at 25 °C. The absorption spectrum of DTABN in *n*-hexane at 25 °C (Figure 3) has a structured part between 35000 and 40000 cm^{-1} and a structureless band between 27000 and 35000 cm^{-1} with a maximum at 31040 cm^{-1}. The structured absorption band of DTABN is similar to that of 4-methylbenzonitrile (4MBN)[52] and CBQ,[19,53−55] which are also included in the Figure. In all three molecules, the lowest-energy peak between 35000 and 40000 cm^{-1} occurs at about the same energy: 35890, 35890, and 35910 cm^{-1}, the energy of the L_b state of the benzonitrile moiety (Table 2).

The absorption of DTABN between 27000 and 40000 cm^{-1} is relatively weak, with an extinction coefficient ϵ^{max} of 1140 M^{-1} cm^{-1} at the lowest-energy maximum and peaks with ϵ = 660 M^{-1} cm^{-1} at 35890 cm^{-1} and ϵ = 760 M^{-1} cm^{-1} at 37425 and 38255 cm^{-1}, see Table 2. The absorption spectrum of 4MBN (Figure 3) shows a more pronounced vibrational structure than that of DTABN, with a smaller ϵ^{max} = 430 M^{-1} cm^{-1} at 37440 cm^{-1}, clearly resembling the structure observed in the spectrum of DTABN. CBQ has larger extinction coefficients than 4MBN and DTABN in this spectral range, with ϵ = 810 M^{-1} cm^{-1} at 35890 cm^{-1} and ϵ = 1000 M^{-1} cm^{-1} at 37105 cm^{-1}, see Figure 3 and Table 2.

The absorption spectrum of CBQ,[53−55] for which the amino nitrogen is effectively decoupled from the rest of the molecule due to its nearly perpendicular twist with respect to the benzonitrile moiety (amino twist angle θ = 88.7°;[50] see below), contains a main structured benzonitrile-like part, with an additional very weak absorption on the red edge of the spectrum (Figure 3). Such an additional red-shifted absorption is much more pronounced in the case of DTABN (Figure 3), which indicates that the di-*tert*-butylamino group in DTABN, although also substantially twisted (75°; see below), is apparently less strongly decoupled from the rest of the molecule than the amino nitrogen of CBQ.

The fluorescence spectrum of DTABN in *n*-hexane at 25 °C consists of a broad band with a maximum at 25630 cm^{-1}, with a fluorescence quantum yield Φ_f of 0.0053 (Table 3). The identification of this emission as originating mainly from an ICT state will be discussed in a later section, where the solvatochromic data of DTABN are presented.

Comparison of the Absorption Spectra of DMABN, DTABN, CBQ, and 4MBN. For a comparison of the strongly twisted DTABN with the effectively planar[48] DMABN, the absorption spectra of these molecules in *n*-hexane are depicted in Figure 4. The absorption spectrum of CBQ in this solvent is also shown. The main band in the spectrum of DMABN, with $\tilde{\nu}^{max}$(abs) = 35625 cm^{-1} (Table 2),[25] is assigned to the $S_0 \rightarrow S_2(L_a,CT)$ transition, whereas the lowest peak at the leading edge of the absorption band of DMABN in Figure 4 (31780 cm^{-1}) is attributed to the $S_1(L_b)$ state.[55,56]

The comparison of the absorption spectra of DTABN and CBQ with that of DMABN in *n*-hexane (Figure 4), reveals that the extinction coefficients ϵ^{max} of DTABN (1140 M^{-1} cm^{-1}) and CBQ (1000 M^{-1} cm^{-1}) are about 25 times smaller than those of DMABN (29370 M^{-1} cm^{-1}, Table 2). As a further difference, the absorption maximum $\tilde{\nu}^{max}$(abs) of DTABN (31040 cm^{-1}) is strongly red-shifted with respect to that of

TABLE 1. Data for the Ground State Structure of 3-(Di-*tert*-butylamino)benzonitrile (mDTABN), 1-*tert*-Butyl-6-cyano-1,2,3,4-tetrahydroquinoline (NTC6), 3,5-Dimethyl-4-(dimethylamino)benzonitrile (MMD), and 4-(Dimethylamino)benzonitrile (DMABN) from X-ray Crystal Analysis Where The Bond Lengths Are in pm (See the Molecular Structure of mDTABN in Figure 1)

	mDTABN[a] (A)	mDTABN[a] (B)	MMD[b]	DMABN[b]		NTC6[c]
N(7)−C(X)[d]	143.7	143.8	141.4	136.5	N(1)−C(9)	137.4
N(7)−C(10)	150.5	150.2	144.1	144.8	N(1)−C(13)	147.6
N(7)−C(14)	150.4	151.1	144.1	144.8	N(1)−C(2)	149.3
C(1)−C(2)	139.7	139.8	138.7	138.8	C(1)−C(13)	140.0
C(1)−C(6)	139.0	138.5	138.7	138.8	C(6)−C(7)	139.1
C(1)−C(8)	144.2	144.4	142.5	142.7	C(6)−C(11)	143.3
C(2)−C(3)	138.9	138.8	138.2	137.0	C(5)−C(10)	137.9
C(3)−C(4)	139.6	139.6			C(9)−C(10)	142.1
C(4)−C(5)	138.6	139.2	140.8	140.0	C(8)−C(9)	141.0
C(5)−C(6)	137.6	138.8	140.8	140.0	C(7)−C(8)	137.8
C(8)−N(9)	114.3	114.5	114.7	114.5	C(11)−N(12)	115.0
C(10)−C(11)	153.4	153.4			C(13)−C(14)	153.9
C(10)−C(12)	153.0	153.4			C(13)−C(15)	152.9
C(10)−C(13)	152.6	152.9			C(13)−C(16)	153.2
C(14)−C(15)	153.0	153.0			C(2)−C(3)	153.9
C(14)−C(16)	154.1	153.1				
C(14)−C(17)	153.8	153.9				
C(X)−N(7)−C(10)[d]	112.2	113.0	118.3	121.5	C(2)−N(1)−C(9)	115.8
C(10)−N(7)−C(14)	115.1	114.3	116.2	116.4	C(2)−N(1)−C(13)	123.4
C(X)−N(7)−C(14)[d]	123.2	123.5	119.2	120.6	C(9)−N(1)−C(13)	119.8
twist angle θ[e]	86.4	86.6	57.4	2.2	twist angle θ[e]	22.7
$\sum N$[f]	350.5	350.8	353.8	358.5	$\sum N$[f]	359.0
pyramidal angle φ[g]	32.4	32.3	24.4	8.6	pyramidal angle φ[g]	9.6
quinoidality[h]	0.9899	0.9964	0.9964	0.9870	quinoidality[h]	0.9907

[a] Data (A) and (B) for two different molecules in the unit cell. The standard deviations are 0.2−0.3 pm for the bond lengths and 0.2° for the angles. [b] Reference 48. [c] Reference 47. [d] $X = 3$ for mDTABN; $X = 4$ for the other molecules. [e] Twist angle: (C(2)C(3)N(7)C(10) + C(4)C(3)N(7)C(14))/2 for mDTABN and similar for the other molecules. [f] Sum of the angles around the amino nitrogen N(7). [g] Pyramidal angle: angle between the vector N(7)-C(*X*) and the plane C(10)N(7)C(14). [h] Quinoidality of the phenyl ring: (C(5)−C(6))/(C(1)−C(6)).

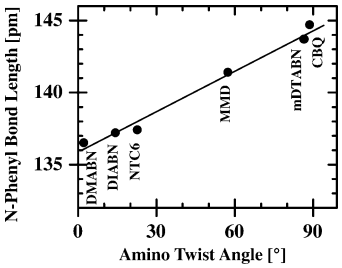

Figure 2. Plot of the amino-phenyl bond length (see Figure 1, Table 1 and text) vs the amino twist angle θ, for a series of aminobenzonitriles (data from Table 1 and refs 22, 49, and 50): 4-(dimethylamino)-benzonitrile (DMABN), 4-(diisopropylamino)benzonitrile (DIABN), 1-*tert*-butyl-6-cyano-1,2,3,4-tetrahydroquinoline (NTC6), 3,5-dimethyl-4-(dimethylamino)benzonitrile (MMD), 3-(di-*tert*-butylamino)benzonitrile (mDTABN), and 6-cyanobenzoquinuclidine (CBQ). The amino−phenyl bond length ranges between that of a double C═N bond (128 pm) and a single CN bond (147 pm), see text.

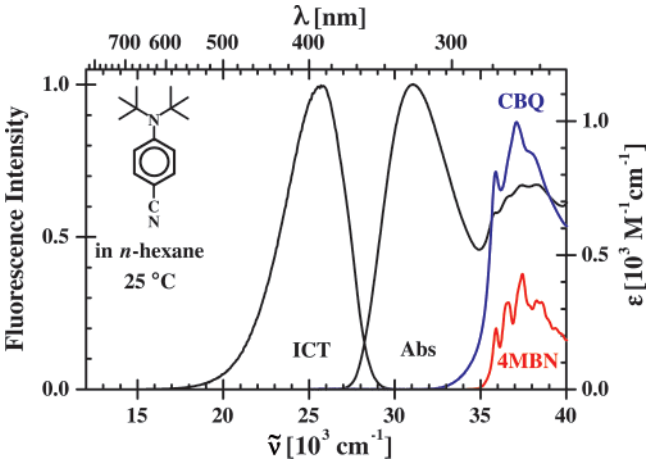

Figure 3. Absorption and fluorescence spectrum of 4-(di-*tert*-butylamino)benzonitrile (DTABN) in *n*-hexane at 25 °C. The absorption spectra of 6-cyanobenzoquinuclidine (CBQ, blue) and 4-methylbenzonitrile (4MBN, red) are also shown for comparison, see text. The excitation wavelength for the fluorescence spectrum of DTABN is 325 nm.

DMABN (35625 cm^{-1}). This red-shift is at first sight surprising, as it could have been expected that by the twisting of the amino group the absorption band should move to higher energies, toward the benzonitrile absorption of a fully decoupled, perpendicularly twisted aminobenzonitrile such as with CBQ. A similar, although smaller, red-shift (to 33090 cm^{-1}) occurs with MMD, having an amino twist angle θ of 57° (Table 1).[48] This shift has been explained by the lowering of the molecular symmetry of MMD as compared with DMABN, which leads to an increased coupling with additional electronic states, forbidden by symmetry in the case of DMABN.[55] This explanation may also hold for DTABN. The appearance of the red-shifted absorption band of DTABN at 31040 cm^{-1} and its near absence in the case of CBQ (Figures 3 and 4) is an indication of the presence of an appreciable electronic coupling between the $-N(tert\text{-butyl})_2$ and benzonitrile groups in DTABN.

DTABN in MeCN. Absorption and Fluorescence Spectra. The absorption and fluorescence spectra of DTABN in MeCN at 25 °C are shown in Figure 5. The unstructured lowest-energy absorption band with a maximum at 30210 cm^{-1} is red-shifted as compared with that in *n*-hexane (Figure 3). The extinction coefficient ϵ^{max} of this band in MeCN (1230 M^{-1} cm^{-1}) is about the same as ϵ^{max} in *n*-hexane (1140 M^{-1} cm^{-1}), see Table 2. The structured absorption of DTABN in MeCN between 35000 and 40000 cm^{-1} resembles that in *n*-hexane, but does not show the red-shift with solvent polarity observed for the broad absorption band.

The fluorescence spectrum of DTABN in MeCN at 25 °C consists of a broad structureless emission with a maximum $\tilde{\nu}^{max}$(flu) at 20900 cm^{-1} and an overall fluorescence quantum yield Φ_f of 0.039 (Table 3). The fluorescence band is red-shifted by 4730 cm^{-1} with respect to the emission maximum of DTABN in *n*-hexane (Figure 3 and Table 3). This large red-shift and also the shape of the fluorescence spectrum indicates that the emission of DTABN in MeCN mainly originates from the ICT state, with perhaps a minor contribution from the

TABLE 2. Data Obtained from the Absorption Spectra of 4-(Di-*tert*-butylamino)benzonitrile (DTABN), 3-(Di-*tert*-butylamino)benzonitrile (mDTABN), 4-Methylbenzonitrile (4MBN), and 6-Cyanobenzoquinuclidine (CBQ) in *n*-Hexane and of DTABN and mDTABN in Acetonitrile (MeCN) at 25 °C

	DTABN		mDTABN				
solvent	*n*-hexane	MeCN	*n*-hexane	MeCN	4MBN *n*-hexane	CBQ *n*-hexane	DMABN *n*-hexane
ϵ^{max} [M^{-1} cm^{-1}] (at $\tilde{\nu}^{max}$)	1140 (31040 cm^{-1}) 760 (37425 cm^{-1}) 760 (38255 cm^{-1})	1230 (30210 cm^{-1}) 940 (38330 cm^{-1})	620 (34090 cm^{-1}) 820 (36580 cm^{-1})	540 (33820 cm^{-1}) 920 (36560 cm^{-1})	430 (37440 cm^{-1})	1000 (37105 cm^{-1})	29370 (35625 cm^{-1})
	660[a] (35890 cm^{-1})	740[a] (35800 cm^{-1})	760[a] (35530 cm^{-1})	790[a] (35460 cm^{-1})	230 (^1L_b)[a] (35910 cm^{-1})	810 (^1L_b)[a] (35890 cm^{-1})	2220 (^1L_b)[a] (31780 cm^{-1})

[a] Lowest-energy peak of the structured part of the absorption spectrum, assigned to the $S_0 \rightarrow S_1(L_b)$ transition in 4MBN, CBQ, and DMABN; see Figures 3−6 and text.

TABLE 3. Data Obtained from the Fluorescence Spectra of 4-(Di-*tert*-butylamino)benzonitrile (DTABN) in *n*-Hexane, Diethyl Ether (DEE), Tetrahydrofuran (THF), and Acetonitrile (MeCN) Solvents and of 3-(Di-*tert*-butylamino)benzonitrile (mDTABN) in *n*-Hexane and MeCN Solvents at 25 °C

	DTABN				mDTABN	
	n-hexane	DEE	THF	MeCN	*n*-hexane	MeCN
ϵ[a]	1.88	4.24	7.39	36.7	1.88	36.7
Φ'(ICT)[b]	0.0053	0.0073	0.014	0.039	0.013	0.027
$\tilde{\nu}^{max}$ (ICT) [cm^{-1}][c]	25 630	23 750	22 710	20 900	26 290	21 280
ICT half-width [cm^{-1}][d]	4210			4365	4195	4770
$E(S_1)^{fl}$ [cm^{-1}][e]	28 260	27 200	26 470	25 480	29 060	26 780
abs(cs) [10^{-17} cm^2][f]	0.19			0.20	0.10	0.089
em(cs) [10^{-17} cm^2][g]	0.15			0.41	0.20	0.083
$\tilde{\nu}^{max}$ (em(cs)) [cm^{-1}][h]	25 350			20 550	26 070	20 880
$E(S_1)^{cs}$ [cm^{-1}][i]	28 200			25 390	28 970	26 580

[a] Dielectric constant. [b] ICT fluorescence quantum yield. The total fluorescence spectrum consists mainly of ICT emission. The precise contribution of the LE emission cannot be established (Figures 3, 5 and 6). [c] ICT emission maximum. [d] Full width at half-maximum of the ICT fluorescence band. For 4-(diisopropylamino)benzonitrile (DIABN), the following ICT half-widths are observed: 4435 cm^{-1} (*n*-hexane), 4355 cm^{-1} (MeCN), ref 22. For 4-(dimethylamino)benzonitrile (DMABN) the half-widths are: in *n*-hexane (LE): 3510 cm^{-1}, in MeCN (ICT): 5090 cm^{-1} (ref 8). [e] Crossing point of the fluorescence and absorption spectra (Figures 3, 5, and 6). [f] Absorption cross section (cs) σ(abs). [g] Emission cross section σ(em). [h] Maxima of the emission cross section spectra. [i] Crossing point of the emission and absorption cross section spectra. The cross section data are employed in the correction procedure for the transient absorption spectra in Figures 10, 11, 13, and 14.

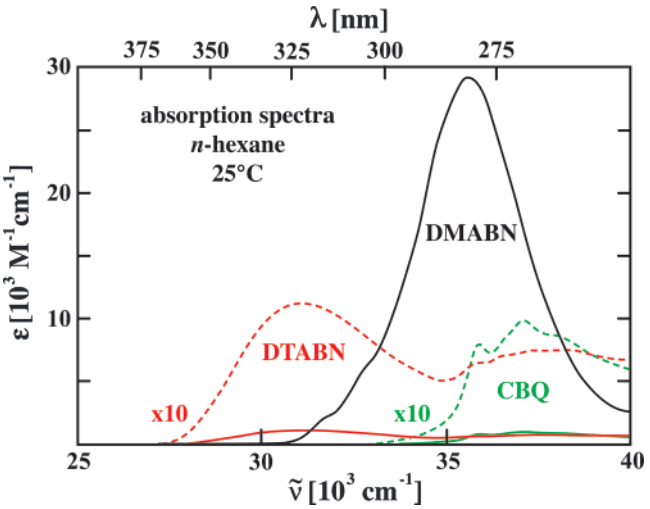

Figure 4. Absorption spectra of 4-(dimethylamino)benzonitrile (DMABN), 4-(di-*tert*-butylamino)benzonitrile (DTABN) and 6-cyanobenzoquinuclidine (CBQ) in *n*-hexane at 25 °C. The dashed spectra (DTABN and CBQ) are multiplied by a factor of 10.

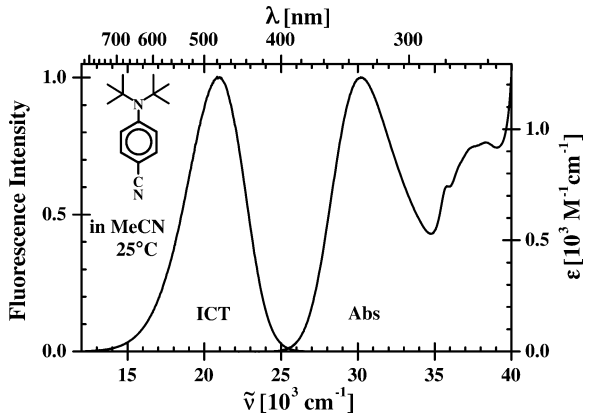

Figure 5. Absorption and fluorescence spectrum of 4-(di-*tert*-butylamino)benzonitrile (DTABN) in acetonitrile (MeCN) at 25 °C. The excitation wavelength for the fluorescence spectrum is 327 nm.

initially excited LE state, similar to what has been found with DIABN and NTC6.[22,24,42] This identification will be further substantiated in a subsequent section on solvatochromic measurements with DTABN.

mDTABN in *n*-Hexane and MeCN at 25 °C. ICT with a Meta-Substituted Aminobenzonitrile. Absorption Spectra. The absorption spectra of mDTABN in *n*-hexane and MeCN at 25 °C (Figure 6) are similar to those of DTABN in these solvents (Figures 3 and 5). The most prominent feature in the absorption spectra of mDTABN is the structured benzonitrile-like absorption between 35000 and 40000 cm^{-1}, with a weaker unstructured band at lower energies. A comparison with the absorption spectra of DTABN and CBQ (Figures 3 and 4) leads to the conclusion that the electronic coupling between the strongly twisted amino and benzonitrile moieties of mDTABN (θ = 86.5°, Figure 1) is smaller than in the case of DTABN, but larger than for CBQ with θ = 88.7° (Table 4).

Fluorescence Spectra. The fluorescence spectra of mDTABN in *n*-hexane and MeCN at 25 °C, with a fluorescence quantum yields Φ_f of 0.013 and 0.027 (Table 3), respectively, consist of

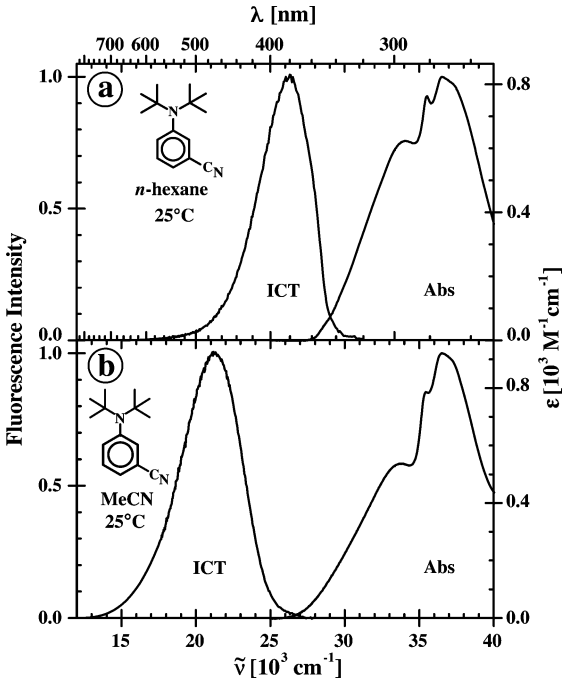

Figure 6. Absorption and fluorescence spectra of 3-(di-*tert*-butylamino)benzonitrile (mDTABN) in (a) *n*-hexane and (b) acetonitrile (MeCN) at 25 °C. The excitation wavelength for the fluorescence spectra is 288 nm for mDTABN in *n*-hexane (a) and 285 nm in MeCN (b).

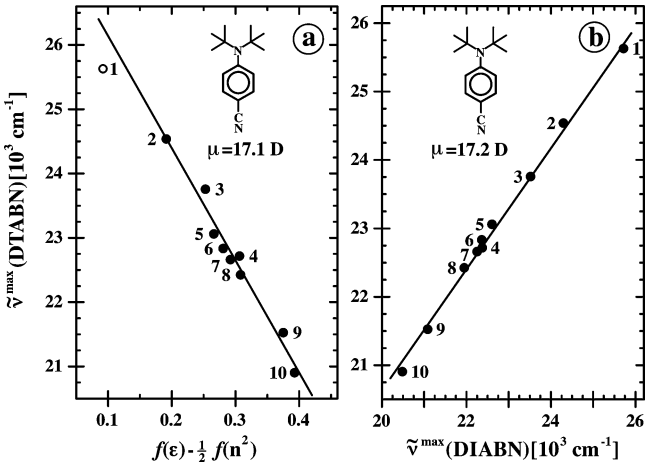

Figure 7. Plots of the ICT fluorescence maxima $\tilde{\nu}^{max}$(ICT) of 4-(di-*tert*-butylamino)benzonitrile (DTABN) in 10 solvents vs (a) the solvent polarity parameter $f(\epsilon) - {}^1/_2 f(n^2)$ and (b) $\tilde{\nu}^{max}$(ICT) of 4-(di-isopropylamino)benzonitrile (DIABN), see eqs 1−3. For the $\tilde{\nu}^{max}$(flu) and the numbering of the solvents, see Table 5. From the slopes of the plots, the ICT dipole moment μ_e(ICT) of DTABN is calculated, 17.1 D for (a) and 17.2 D for (b); see eq 1 and text. Point 1 in part a is not included in the analysis.

a broad band without evidence for dual emission. The fluorescence maximum $\tilde{\nu}^{max}$(flu) undergoes a red-shift from 26290 cm^{-1} in *n*-hexane to 21280 cm^{-1} in MeCN. This red-shift of 5010 cm^{-1}, similar to that (4730 cm^{-1}) found for DTABN (Figures 3 and 5), indicates that also with mDTABN an ICT reaction takes place. This is the first example of such a reaction for a meta-substituted aminobenzonitrile.[11,27−32] Further evidence for the ICT character of the fluorescence spectra of mDTABN will be presented in a later section where solvatochromic measurements are discussed.

Amino Twist Angle of DTABN from Absorption Spectra. As can be seen from the data for a series of aminobenzonitriles and CBQ in *n*-hexane at 25 °C in Table 4, there is a clear correlation between the extinction coefficient ϵ^{max} of the maximum of the lowest-energy absorption band and the amino twist angle θ determined from X-ray crystal analysis, as previously discussed in the literature.[25,57,58] By using this somewhat empirical correlation, a twist angle of 75° is calculated for DTABN from its ϵ^{max} in *n*-hexane (Table 4).[59] From a comparison of ϵ^{max} for DTABN with that of DMABN in *n*-hexane (Table 4), an amino twist angle θ of 78.6° is calculated, by employing the well-established relation $\cos^2\theta = \epsilon^{max}(\text{DTABN})/\epsilon^{max}(\text{DMABN})$ and $\theta = 0$ for DMABN.[25,57,58]

Support for our finding that the twist angle θ of DTABN (75°) is smaller than that of mDTABN (86.5°), comes from a comparison of the absorption spectra of DTABN (Figures 3 and 5) and mDTABN (Figure 6). The smaller amino twist and hence larger electronic coupling between the amino and benzonitrile groups in DTABN as compared with mDTABN, is reflected in the larger extinction coefficient ϵ^{max} for DTABN than for mDTABN of the lowest-energy absorption band, i.e., the amino/benzonitrile coupling in mDTABN is in this respect closer to CBQ than to DTABN (Figures 3−6).

The broad absorption band of mDTABN in *n*-hexane at lower energy than the benzonitrile-like absorption band is less red-

TABLE 4. Extinction Coefficients ϵ^{max} of the Lowest-Energy Absorption Maxima in *n*-Hexane at 25 °C and the Amino Twist Angles θ from X-ray Crystal Analysis, for Aminobenzonitriles and 6-Cyanobenzoquinuclidine (CBQ)

	ϵ^{max} [M^{-1} cm^{-1}]a	λ^{max} [nm][a]	θ[deg][b]
DMABN[c]	29 370	280.7	0
DIABN[d]	25 560	287.7	14
NTC6[e]	22 085	299.7	22.7
MMD[f]	5100	302.0	59
mDTABN[g]	590	293.4	86.5
CBQ[h]	58[i]	294[i]	88.7
DTABN[j]	1140	322.2	75[k]

[a] Data for DMABN, mDTABN, CBQ, and DTABN from Table 2. Data for DIABN and NTC6 from ref 25 and for MMD from ref 58. [b] Data for DMABN and MMD from ref 48, for DIABN from refs 22 and 49, for NTC6 from ref 25, for mDTABN from Table 2 and for CBQ from ref 50. [c] 4-(Dimethylamino)benzonitrile. [d] 4-(Diisopropylamino)benzonitrile. [e] 1-*tert*-butyl-6-cyano-1,2,3,4-tetrahydroquinoline. [f] 3,5-Dimethyl-4-(dimethylamino)benzonitrile. [g] 3-(Di-*tert*-butylamino)benzonitrile. [h] 6-Cyanobenzoquinuclidine. [i] Data not for a maximum in the absorption spectrum; see Figures 3 and 4. [j] 4-(Di-*tert*-butylamino)benzonitrile. [k] Calculated from the correlation between ϵ^{max} and θ.

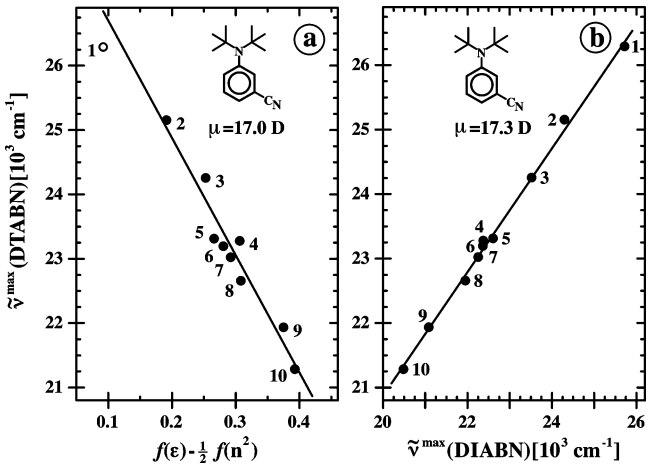

Figure 8. Plots of the ICT fluorescence maxima $\tilde{\nu}^{max}$(ICT) of 3-(Di-*tert*-butylamino)benzonitrile (mDTABN) in 10 solvents (Table 3) vs (a) the solvent polarity parameter $f(\epsilon) - {}^1/_2 f(n^2)$ and (b) $\tilde{\nu}^{max}$(ICT) of 4-(di-isopropylamino)benzonitrile (DIABN), see eqs 1−3. For the $\tilde{\nu}^{max}$(flu) and the numbering of the solvents, see Table 5. From the slopes of the plots, the ICT dipole moment μ_e(ICT) of DTABN is calculated, (a) 17.0 D and (b) 17.3 D; see eq 1 and text. Point 1 in part a is not included in the analysis.

TABLE 5. ICT Emission Maxima in 1000 cm^{-1} of 4-(Di-*tert*-butylamino)benzonitrile (DTABN), 3-(Di-*tert*-butylamino)benzonitrile (mDTABN), and 4-(Diisopropylamino)benzonitrile (DIABN) in a Series of Solvents Spanning the Polarity Scale $f(\epsilon) - {}^1/_2 f(n^2)$ (eqs 2 and 3)

solvent	ϵ	n	$f(\epsilon)$	$f(n^2)$	$f(\epsilon) - {}^1/_2 f(n^2)$	DTABN	mDTABN	DIABN
n-hexane (1)	1.88	1.372	0.185	0.185	0.092	25.63	26.29	25.72
di(*n*-butyl) ether (2)	3.05	1.397	0.289	0.194	0.192	24.53	25.15	24.30
diethyl ether (3)	4.24	1.350	0.342	0.177	0.253	23.75	24.25	23.52
tetrahydrofuran (4)	7.39	1.405	0.405	0.197	0.307	22.71	23.28	22.38
n-butyl acetate (5)	4.95	1.392	0.362	0.192	0.266	23.06	23.31	22.61
n-propyl acetate (6)	5.52	1.382	0.375	0.189	0.281	22.83	23.19	22.37
ethyl acetate (7)	5.99	1.370	0.384	0.184	0.292	22.66	23.02	22.26
methyl acetate (8)	6.88	1.358	0.398	0.180	0.308	22.42	22.66	21.96
n-propyl cyanide (9)	24.2	1.382	0.470	0.189	0.375	21.52	21.93	21.09
acetonitrile (10)	36.7	1.342	0.480	0.174	0.393	20.90	21.28	20.49

TABLE 6. Data from the Solvatochromic Analysis of the Fluorescence Emission Maxima $\tilde{\nu}^{max}$ of 4-(Di-*tert*-butylamino)-benzonitrile (DTABN) and 3-(Di-*tert*-butylamino)benzonitrile (mDTABN)

	ρ [Å][a]	μ_g [D][b]	slope	μ_e [D][c]
DTABN (eq 1)	4.89	5.2[d]	-17500 ± 1500[e]	17.1 ± 0.4
DTABN (vs DIABN)[f]	4.89 (4.68)	5.2[d] (6.8)	0.90 ± 0.02[g]	17.2 ± 0.2 (18)
mDTABN (eq 1)	4.89	4.5[d]	-18200 ± 1700[h]	17.0 ± 0.7
mDTABN (vs DIABN)[c]	4.89 (4.68)	4.5[d] (6.8)	0.97 ± 0.02[i]	17.3 ± 0.1 (18)

[a] Onsager radius (eq 1), determined from a density equal to 0.78, based on DMABN (ref 60). [b] Ground state dipole moment. [c] Excited-state dipole moment (eq 1). [d] Calculated by AM1; result scaled by μ_g (DMABN) = 6.6 D (ref 11). [e] For plot of $\tilde{\nu}^{max}$ (DTABN) vs $g(\epsilon,n) = f(\epsilon) - {}^1/_2 f n^2$), eqs 1−3, see Figure 7a. [f] For DIABN, ρ = 4.68 Å, μ_g = 6.8 D, μ_e(ICT) = 18 D, from refs 22, 42, and 60. [g] For plot of $\tilde{\nu}^{max}$ (DTABN) vs $\tilde{\nu}^{max}$ (DIABN), see Figure 7b. [h] For plot of $\tilde{\nu}^{max}$ (mDTABN) vs $g(\epsilon,n)$, eqs 1−3, see Figure 8a. [i] For plot of $\tilde{\nu}^{max}$ (mDTABN) vs $\tilde{\nu}^{max}$ (DIABN), see Figure 8b.

shifted (34090 as compared with 31040 cm^{-1}) and weaker (620 as compared with 1140 M^{-1} cm^{-1}) than in the case of DTABN (see Figures 3 and 6 and Table 2). A similar observation is made for mDTABN and DTABN in MeCN (Table 2).

Solvatochromic Measurements. ICT Dipole Moment of DTABN and mDTABN. To determine the excited-state dipole moment μ_e of the molecules DTABN and mDTABN, the energies $\tilde{\nu}^{max}$(flu) of the maxima of their emission bands (Table 5) are plotted against the solvent polarity parameter $g(\epsilon,n) = f(\epsilon) - {}^1/_2 f(n^2)$; see eqs 1−3, where ϵ is the dielectric constant, n the refractive index and ρ the Onsager radius of the solute.[24,42,60]

$$\tilde{\nu}^{max}(\text{flu}) = -\frac{1}{2hc\rho^3}\mu_e(\mu_e - \mu_g)g(\epsilon,n) + \text{const} \qquad (1)$$

$$f(\epsilon) = \frac{(\epsilon - 1)}{(2\epsilon + 1)} \qquad (2)$$

$$f(n^2) = \frac{(n^2 - 1)}{(2n^2 + 1)} \qquad (3)$$

μ_e(ICT) from Solvatochromic Plots for DTABN. The maxima $\tilde{\nu}^{max}$(flu) of the fluorescence band of DTABN (Figures 3 and 5, Table 3) in ten solvents at 25 °C (Table 5) are plotted in Figure 7a against the solvent polarity parameter $f(\epsilon) - {}^1/_2 f(n^2)$, see eqs 1−3. It is seen that $\tilde{\nu}^{max}$(flu) in *n*-hexane (no. 1) somewhat deviates from the least-squares line for the other solvents. From the slope of this line (eq 1, Table 6), a dipole moment of 17.1 D is calculated. In Figure 7b, the maxima $\tilde{\nu}^{max}$(flu) of DTABN are plotted vs the ICT emission maxima of DIABN (Table 5). By employing this procedure, the scatter in the data points is generally reduced by mutually compensating the specific solute/solvent interactions.[24,60] Now, all data points can be fitted by a single line, leading (eq 1) to a dipole moment of 17.2 D, in very good agreement with the outcome from Figure 7a (Table 6). It can now be concluded that the fluorescence of DTABN originates from the ICT state for all solvents investigated, from *n*-hexane (Figure 3) to MeCN (Figure 5). In these fluorescence spectra, an LE emission cannot be identified with certainty. This lack of LE fluorescence is due to the extremely short (subpicosecond) decay time of the LE state, which can be observed by femtosecond transient absorption measurements to be presented in a later section. The μ_e(ICT) of 17 D obtained here for DTABN is similar to that of DMABN (17 D), DIABN (18 D) and NTC6 (19 D).[11,22,24,60]

TABLE 7. ICT Fluorescence Decay Times τ_1, Equal to τ'_0(ICT), and Radiative Rate Constant k'_f(ICT) (Scheme 2), of 4-(Di-*tert*-butylamino)benzonitrile (DTABN) and 3-(Di-*tert*-butylamino)benzonitrile (mDTABN) in Solvents of Different Polarity at Various Temperatures from Picosecond Fluorescence Decays at the Emission Wavelength λ_{em} (Figures 3, 5, and 6)

solvent	T [°C]	λ_{em} [nm]	τ_1 [ns]	k'_f(ICT) [10^7 s^{-1}]
n-hexane	25	395	0.863[b]	0.62[b]
($\epsilon^{25} = 1.88$)	25	390	1.53[c]	0.86[c]
	−95	390	0.847[b]	
diethyl ether	25	475	1.46[b]	0.52[b]
($\epsilon^{25} = 4.24$)	−65	450	1.91[b]	
	−105	470	2.43[b]	
tetrahydrofuran	25	440	2.37[b]	0.59[b]
($\epsilon^{25} = 7.39$)	−45	440	2.87[b]	
	−105	440	3.23[b]	
acetonitrile	25	520	3.48[b]	1.1[b]
($\epsilon^{25} = 36.7$)	25	490	10.5[c]	0.26[c]
	−45	520	3.59[b]	

[a] Determined from τ'_0(ICT) and the ICT fluorescence quantum yields Φ'(ICT) in Table 3: k'_f(ICT) = Φ'(ICT)/τ'_0(ICT). [b] DTABN. [c] mDTABN.

μ_e(ICT) from Solvatochromic Plots for mDTABN. The maxima $\tilde{\nu}^{max}$(flu) of the fluorescence bands of mDTABN in ten solvents at 25 °C (Table 5) are plotted against the solvent polarity parameter $f(\epsilon) - {}^1/_2 f(n^2)$ in Figure 8a (eqs 1−3) and vs the ICT emission maxima of DIABN in Figure 8b. From the slopes of these plots, dipole moments of 17.0 D (Figure 8a, excluding *n*-hexane) and 17.3 D (Figure 8b) are calculated (Table 6). These results show that the fluorescence of mDTABN in *n*-hexane as well as in MeCN (Figure 6) originates from an ICT state, similar to what was found for DTABN (Figure 7). It is therefore concluded that mDTABN undergoes an ICT reaction even in a nonpolar alkane solvent such as *n*-hexane. The ICT with mDTABN is the first example of such a reaction for a meta-substituted aminobenzonitrile.[11,27−32]

Picosecond SPC Measurements of DTABN. The picosecond SPC fluorescence decays of DTABN measured near the ICT

TABLE 8. Excited State Absorption (ESA) Maxima, the ICT Reaction Time τ_3, and the Solvent Cooling Time τ_2 (eq 4) for 4-(Di-*tert*-butylamino)benzonitrile (DTABN) and the ESA Maxima for 4-(Dimethylamino)benzonitrile (DMABN) in *n*-Hexane and Acetonitrile (MeCN)

	ESA maxima [nm]		decay times τ_3 and τ_2 [fs]	
	n-hexane	MeCN	*n*-hexane[a]	MeCN[b]
DTABN (0.1 − 2.0 ps)[c]	316, 425 (Figure 10b)	318, 425 (Figure 13b)	70 (τ_3, Figure 10)	60 (τ_3, Figure 13)
(1 − 60 ps)[c]	316, 425 (Figure 11b)	318, 425 (Figure 14b)	70 (τ_3, Figure 11) 2200 (τ_2, Figure 11c) 6900 (τ_2, Figure 11d)	90 (τ_3, Figure 14c)[d] 12000 (τ_2, Figure 14c,d)
DMABN	300, 320, 445, 470, 745 (LE), Figure 12a	315, 425, (490), 970 (ICT), Figure 12c		

[a] Decay time $\tau_1 = 0.86$ ns (τ'_0(ICT), Figure 10a). [b] Decay time $\tau_1 = 3.48$ ns (τ'_0(ICT), Figure 10c). [c] Pump−probe delay time. [d] In Figure 14d (delay time 1 − 60 ps) $\tau_3 = 100$ fs.

SCHEME 2. ICT Reaction Scheme

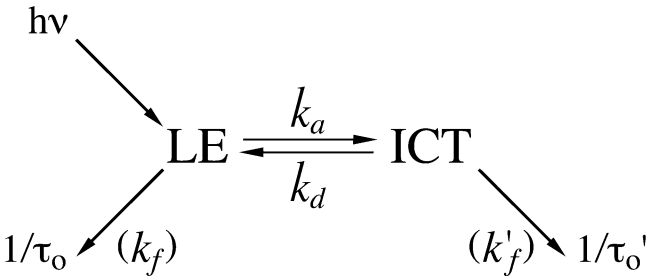

emission maximum (Figures 3 and 5) at various temperatures can be fitted with two exponentials in *n*-hexane, whereas in DEE, THF, and MeCN the decays are single exponential (Figure 9 and Table 7). For DTABN in *n*-hexane at 25 °C (Figure 9a), the decay time of 2.62 ns is attributed to an impurity, as DTABN is somewhat unstable in solution. The short (subpicosecond) decay times resulting from the femtosecond transient absorption measurements with DTABN in *n*-hexane and MeCN (see below) could not be detected in psec fluorescence decays with 10.38 ps/channel (Figure 9), nor in those with 0.5 ps/channel (not shown). In analogy with the SPC experiments with DMABN and NTC6,[8,24] the decay time τ_1 is taken to be equal to the lifetime of the ICT state τ'_0(ICT), see Scheme 2. It is found that τ'_0(ICT) becomes longer with increasing solvent polarity (Table 7). The same trend is observed with mDTABN, for which τ'_0(ICT) increases from 1.53 ns in *n*-hexane to 10.48 ns in MeCN (Table 7). The radiative rate constants k'_f(ICT) ($= \Phi'$(ICT)/τ'_0(ICT)) of DTABN and mDTABN, with values between 0.3 and 1.1 × 10^7 s^{-1} (Table 7), are of the same magnitude (0.79 × 10^7 s^{-1})[8] as that of DMABN in MeCN at 25 °C.[31]

In the general Scheme 2, k_a and k_d are the rate constants of the forward and backward ICT reaction, τ_0(LE) and τ'_0(ICT) are the fluorescence lifetimes and k_f(LE) and k'_f(ICT) are the radiative rate constants.

Femtosecond Transient Absorption Spectra of DTABN in *n*-Hexane and Acetonitrile. DTABN in *n*-Hexane. The transient and excited-state absorption (ESA) spectra of DTABN in *n*-hexane over the spectral range 272−692 nm are presented for pump−probe delay times from 0.1 to 2.0 ps in Figure 10, parts a and b, as well as from 1 to 60 ps in Figure 11, parts a and b. The ESA spectra are obtained from the transient absorption spectra by subtracting the bleaching and stimulated emission, employing the cross section data listed in Table 3.[8] The ESA spectrum with a main peak at 316 nm and a smaller absorption maximum around 425 nm resembles that of the ICT state of DMABN in MeCN (Figure 12), which has a major peak at 315 nm and a much lower maximum at 425 nm.[8]

In the case of DMABN in *n*-hexane (Figure 12), the LE absorption maxima are observed between 300 and 320 nm and around 445 and 745 nm.[8] Although there is no clear sign of these LE absorption peaks in the ESA spectrum of DTABN, the broadening of its main absorption band (272−370 nm) and the spectral decay between 510 and 690 nm is attributed to the simultaneous rise of the ICT and the decay of the LE absorption.

A spectral growing-in occurs in the ESA spectra at the short delay times (0.07−2.6 ps) between 334 and 390 nm (Figure 10c), with a shortest time τ_3 of 70 fs for the band integral BI(334,390).[61] This growing-in is due to the rise of the ICT absorption. For the decay of the corresponding BI(510,690) in Figure 10d, the decrease of the LE absorption caused by the LE → ICT reaction, two times are needed for the fitting: $\tau_3 =$ 70 fs and $\tau_2 = 880$ fs. The offset with amplitude A_0 (eq 4)[61] in Figures 10c and 10d, reflects the ICT lifetime τ'_0(ICT) (0.86 ns) of DTABN in *n*-hexane (Figure 9a).

$$\Delta\mathrm{OD} = A_3\exp(\tau_3/t) + A_2\exp(\tau_2/t) + A_1\exp(\tau_1/t) + A_0 \quad (4)$$

The transient absorption and ESA spectra for the long delay times between 1 and 60 ps (Figure 11, parts a and b) remain practically unchanged after 15 ps. From the BI(300,322), growing-in times 70 fs and 2.2 ps are obtained (Figure 11c). Similar decay times (70 fs and 6.9 ps) are measured for BI(344,390), see Figure 11d. Whereas the short decay time τ_3 = 70 fs is again due to the ICT reaction of DTABN (Scheme 2) as was also concluded from the ESA spectra for 0.07−2.6 ps after excitation, the time τ_2 of 6.9 ps (Figure 11d) is ascribed to vibrational cooling, which phenomenon was also found for DMABN and NTC6.[8,25]

Although already for the shortest pump−probe delay time of 100 fs (Figure 10b) the ESA spectrum of DTABN in *n*-hexane is basically that of the ICT state, the growing between 334 and 390 nm is attributed to the ICT reaction from the initially excited LE precursor (Scheme 2). The decay of the LE state ($\tau_3 = 70$ fs) is observed for BI(334,390) for the delay times (0.07−2.6 ps) in Figure 10c and for BI(344,390) for both the delay times (0.07−60 ps) in Figure 11d, as well as for BI(510,690) in Figure 10d.

DTABN in MeCN. The transient and ESA spectra of DTABN in MeCN over the spectral range 272−692 nm are shown for pump−probe delay times between 0.1 and 2.0 ps (Figure 13) and for delay times between 1 and 60 ps (in Figure 14). The ESA spectrum with a main peak at 318 nm and a smaller absorption maximum around 425 nm resembles that of the ICT state of DMABN in MeCN (Figure 12c), which has a major peak at 315 nm and a much weaker maximum at 425 nm.[8] The ESA spectrum of DTABN in MeCN is similar to that

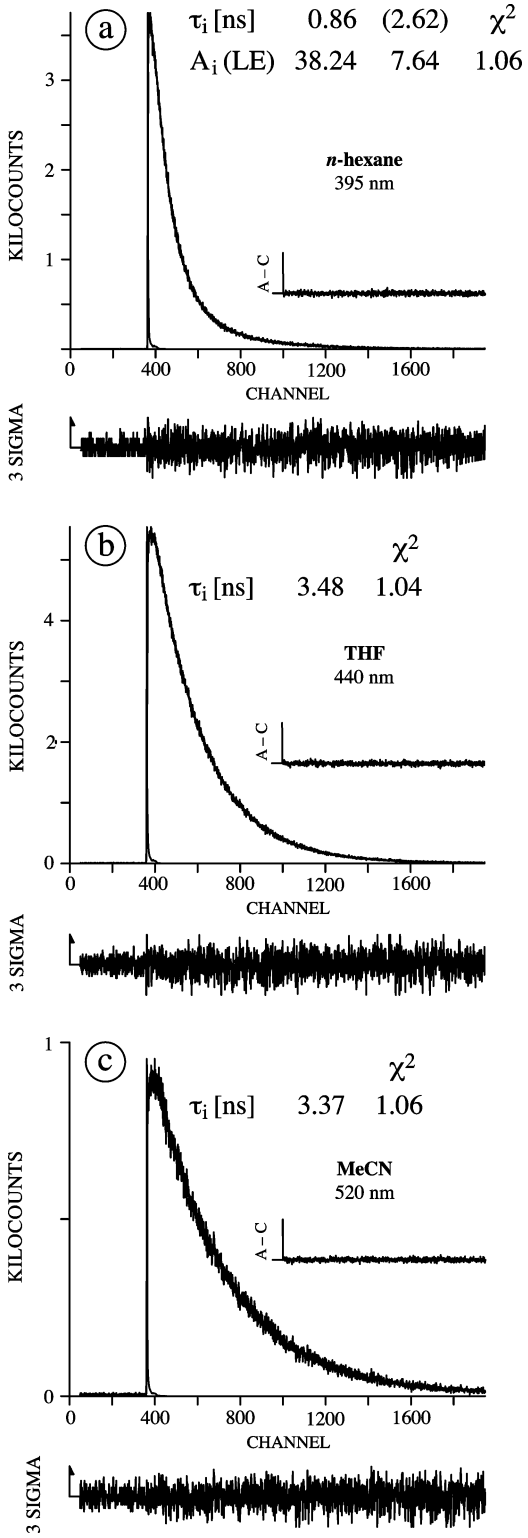

Figure 9. Picosecond fluorescence decays of 4-(di-*tert*-butylamino)-benzonitrile (DTABN) in (a) *n*-hexane, (b) tetrahydrofuran (THF) and (c) acetonitrile (MeCN) at 25 °C. The emission wavelengths λ_{em} are: (a) 395 nm, (b) 440 nm and (c) 520 nm, near the ICT emission maximum of DTABN, see Figures 3 and 5. Excitation wavelength: 272 nm.

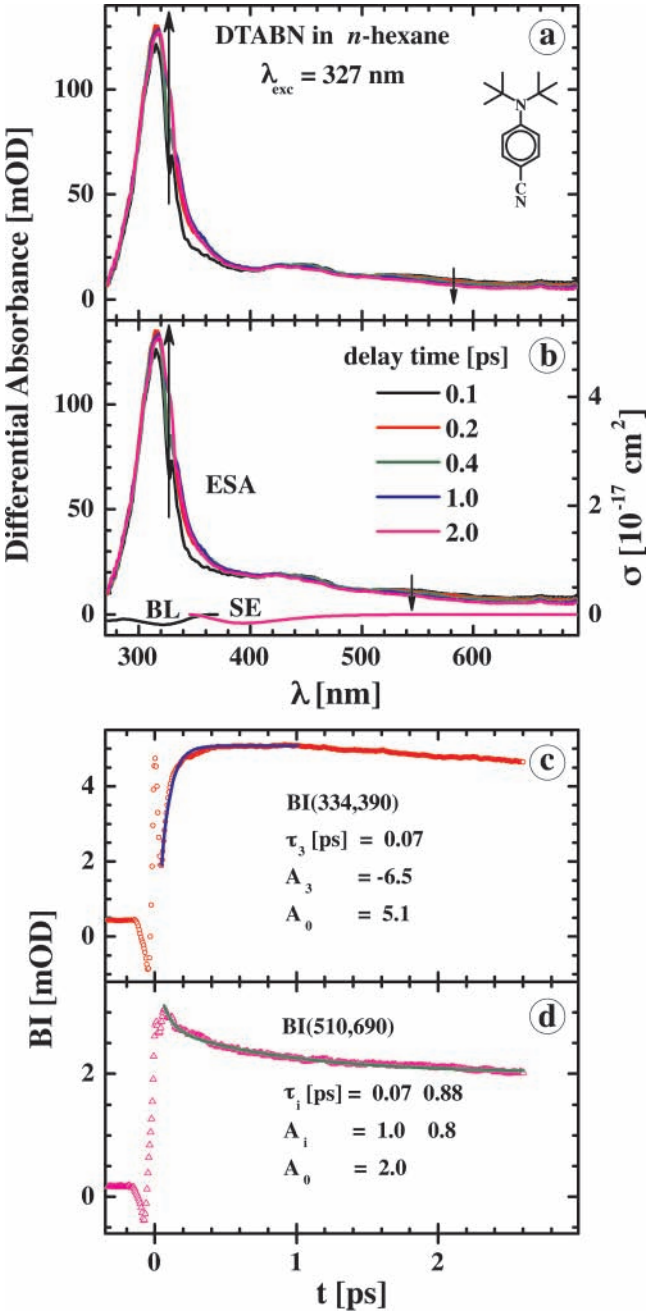

Figure 10. 4-(Di-*tert*-butylamino)benzonitrile (DTABN) in *n*-hexane for short pump−probe delay times (0.1−2.0 ps). (a) Transient absorption spectra (272−692 nm) and (b) excited-state absorption (ESA) spectra after correcting for bleaching (BL) and stimulated emission (SE). The BL and SE spectra are also shown. In parts a and b, the upward arrow (330 nm) indicates the rise of the ICT absorption, whereas the downward arrow (600 nm) shows the decay of the LE absorption. (c) Growing-in of the band integral BI(334,390) between 334 and 390 nm in the ESA spectrum, with decay time $\tau_3 = 0.07$ ps, amplitude A_3 and offset A_0 (eq 4). (d) Decay of the band integral BI(510,690), with decay times $\tau_3 = 0.07$ ps and $\tau_2 = 0.88$ ps. The amplitudes are A_3, A_2, and offset A_0 (eq 4). Excitation wavelength: 327 nm. mOD is the optical density/1000.

in *n*-hexane (Figures 10 and 11), although the 425 nm band in MeCN is more pronounced than in *n*-hexane.

The band integrals BI(390,460) and BI(460,600) of the DTABN spectra for short delay times can be fitted simultaneously with two decay times 60 fs (τ_3) and 760 fs (τ_2), see Figure 13c). From a comparison of the ESA spectrum of DTABN with the LE and ICT spectra of DMABN (Figure 12), it is seen that the spectral range 460−600 nm belongs to the LE state, whereas the range 390−460 nm is part of the ESA spectrum of the ICT state. The double exponential decay of BI(460,600) in Figure 13c is hence attributed to the LE → ICT reaction of DTABN (Scheme 2). Correspondingly, BI(390,460) shows the growing-in of the ICT absorption, with a time τ_3 of 60 fs and a negative amplitude A_3. The same rise time of 60 fs

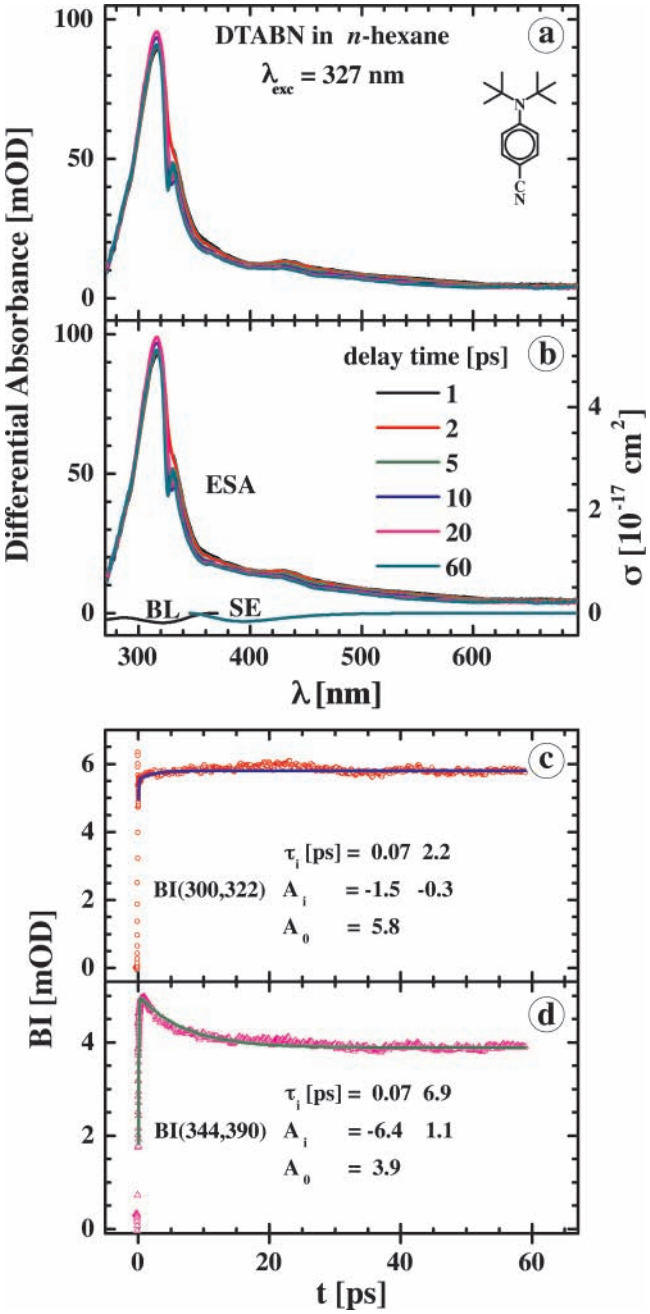

Figure 11. 4-(Di-*tert*-butylamino)benzonitrile (DTABN) in *n*-hexane for long pump−probe delay times (1−60 ps). (a) Transient absorption spectra (272−692 nm) and (b) excited-state absorption (ESA) spectra after correcting for bleaching (BL) and stimulated emission (SE). The BL and SE spectra are also shown. (c) Growing-in and decay of the band integral BI(300,322) between 300 and 322 nm in the ESA spectrum, with decay times τ_3 of and τ_2 of 70 fs and 2.2 ps, with amplitudes A_3 and A_2 and an offset A_0 (eq 4). Excitation wavelength: 327 nm. mOD is the optical density/1000.

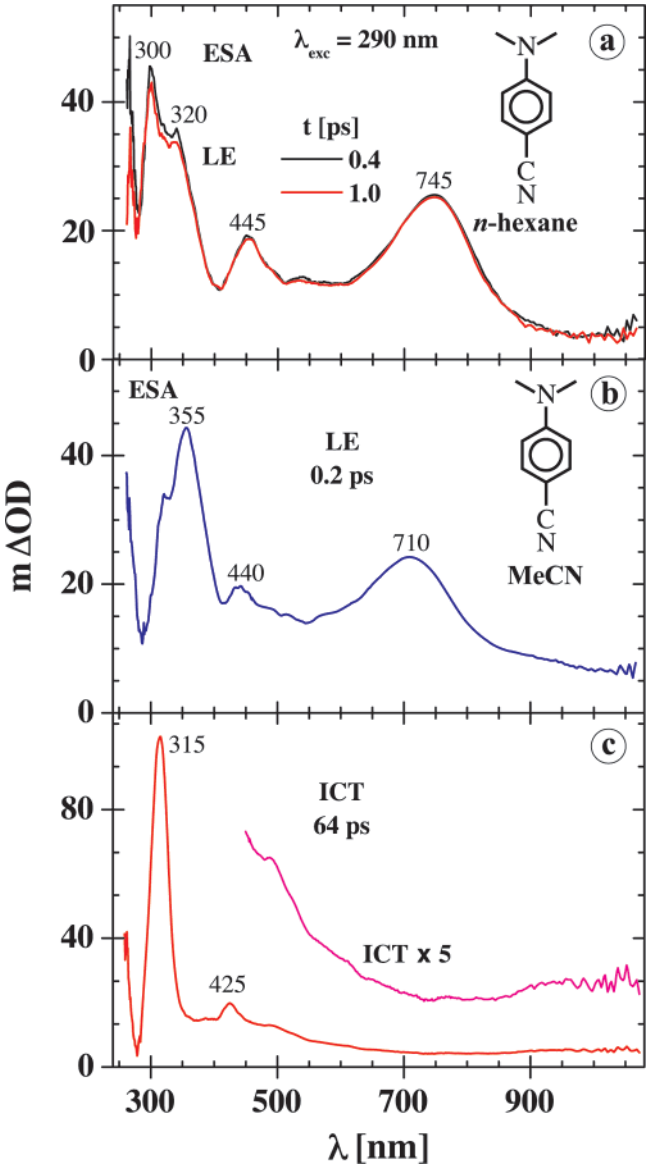

Figure 12. Excited-state absorption (ESA) spectra (260−1040 nm) of 4-(dimethylamino)benzonitrile (DMABN) at 290 nm excitation. (a) In *n*-hexane for two pump−probe delay times (0.4 and 1.0 ps). The spectra are for the LE state of DMABN. (b and c) The ESA spectra in acetonitrile (MeCN) for two pump−probe delay times, (b) 0.2 ps for the LE state and (c) 64 ps for the ICT state. mΔOD is the change in optical density/1000. The figure is adapted from ref 8.

is found for BI(310,365) in Figure 13d. The offset with amplitude A_0 (eq 4) in Figures 13c and 13d is again, as in the case of DTABN in *n*-hexane (Figure 10), connected with the ICT lifetime τ'_0(ICT) of 3.48 ns for DTABN in MeCN (Table 7 and Figure 9c).

The ESA spectra of DTABN in MeCN for the long delay times between 1 and 60 ps (Figure 14a−d) show a growing-in for BI(300,325), with a time τ_3 of 90 fs and a longer time τ_2 of 12 ps (Figure 14c). Whereas τ_3 is attributed to the LE → ICT reaction, as was also concluded above from the time dependence of the ESA spectra between 0.05 and 2.6 ps after excitation (Figure 13, parts c and d), the time τ_2 of 12 ps is assigned to vibrational cooling, similar as in the case of DTABN in *n*-hexane discussed above. For this cooling process, times of around 10 ps have been reported in the literature.[8,25,62]

LE → ICT Reaction of DTABN in *n*-Hexane and MeCN. Although the ESA spectrum of DTABN in *n*-hexane as well as MeCN resembles that of the ICT state already for the shortest pump−probe delay time of 100 fs, the growing-in with 70 fs of BI(330,390) for *n*-hexane (Figure 10c) and that of BI(310,365) and BI(390,460) with 60 fs for MeCN (Figure 13, parts c and d) is due to the rise of the absorption of the ICT state formed from the initially excited LE precursor (Scheme 2). The decay of the LE state with 70 fs in *n*-hexane and with 60 fs in MeCN, is seen from BI(510,690) in Figure 10d and from BI(460,600) in Figure 13c, respectively. The decay time of 60 fs of DTABN in MeCN is the same as found for a series of tetrafluoroaminobenzonitriles in this solvent,[42] in both cases limited by the dielectric relaxation of the solvent.

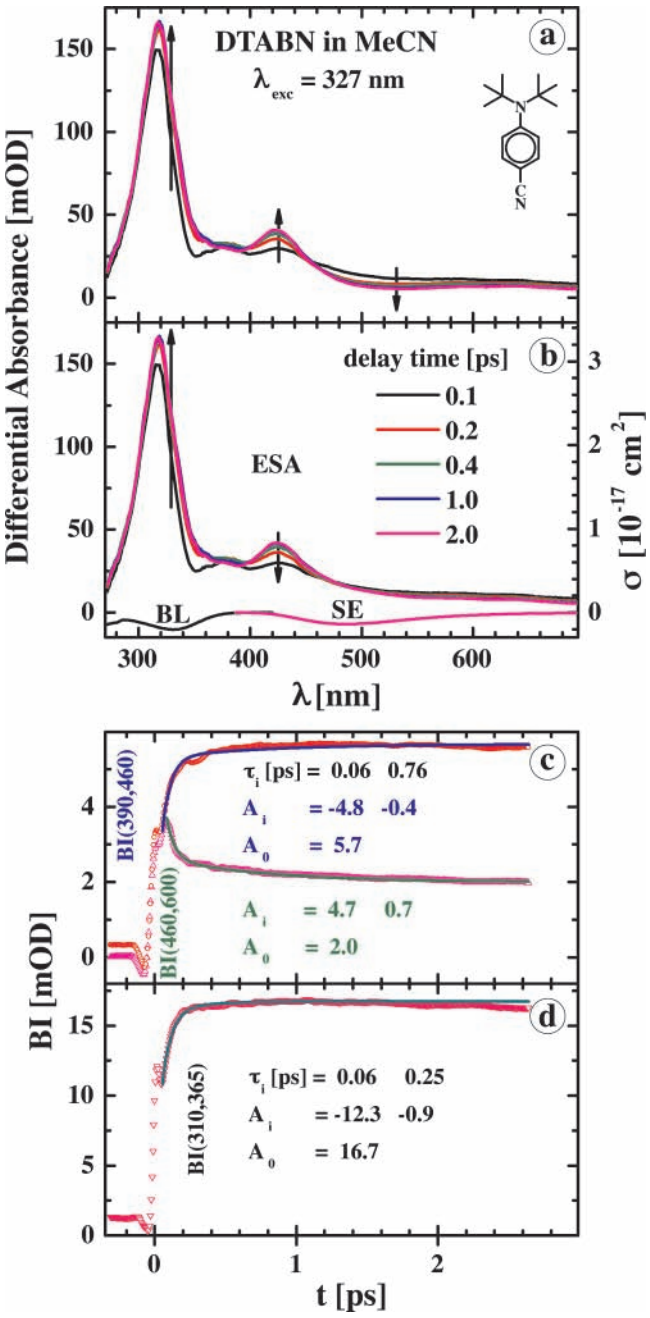

Figure 13. 4-(Di-*tert*-butylamino)benzonitrile (DTABN) in acetonitrile (MeCN) for short pump−probe delay times (0.1−2.0 ps). (a) Transient absorption spectra (272−692 nm) and (b) excited-state absorption (ESA) spectra after correcting for bleaching (BL) and stimulated emission (SE). The BL band and the SE spectrum are also shown. In parts a and b, the upward (318 and 425 nm) arrows indicate the rise of the ICT absorption, whereas the downward arrow (560 nm) shows the decay of the LE absorption, see text. (c) Growing-in of the band integral BI(390,460) between 390 and 460 nm in the ESA spectrum and decay of BI(460,600), fitted simultaneously with the two decay times τ_3 (60 fs) and τ_2 (760 fs), amplitudes A_3 and A_2 and an offset A_0 (eq 4), A_2 is negative (growing-in). BI(390,460) shows the rise of the ICT absorption, BI(460,600) is attributed to the decay of the LE absorption. (d) Growing-in of BI(460,600), fitted with two decay times τ_3 (60 fs) and τ_2 (250 fs), amplitudes A_3 and A_2, and an offset A_0 (eq 4). Excitation wavelength: 327 nm. mOD is the optical density/1000.

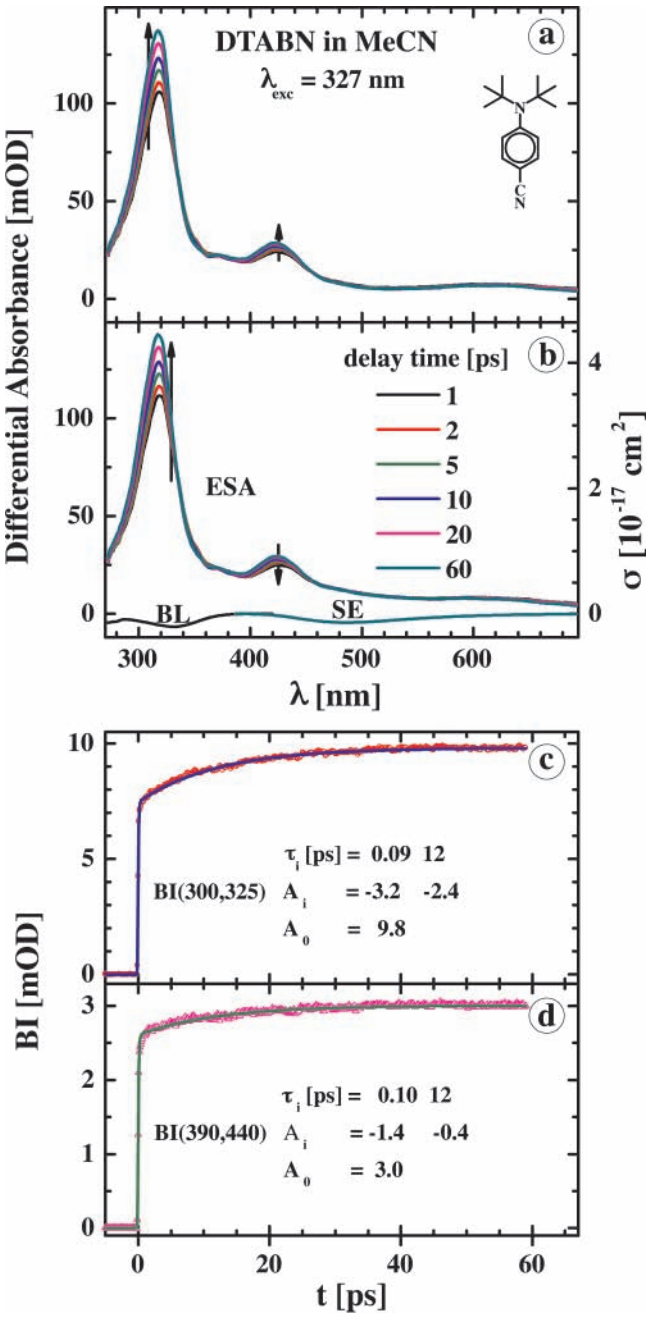

Figure 14. 4-(Di-*tert*-butylamino)benzonitrile (DTABN) in acetonitrile (MeCN) for long pump−probe delay times between 1 and 60 ps. (a) Transient absorption spectra (272−692 nm) and (b) excited-state absorption (ESA) spectra after correcting for bleaching (BL) and stimulated emission (SE). The BL band and the SE spectrum are also shown. In parts a and b, the upward (318 and 425 nm) arrows indicate the rise of the ICT absorption, of which the long time τ_2 of 12 ps is attributed to vibrational solvent cooling. (c) Growing-in of the band integral BI(300,325) between 300 and 325 nm in the transient spectrum. BI(300,325) is fitted with two decay times, τ_3 (90 fs) and τ_2 (12 ps), with amplitudes A_3, A_2, and an offset A_0 (eq 4). (d) Growing-in of the band integral BI(390,440), fitted with two decay times τ_3 (100 fs) and τ_2 (12 ps), with amplitudes A_3, A_2, and an offset A_0 (eq 4). Excitation wavelength: 327 nm. mOD is the optical density/1000.

Possible Structure of the ICT State of DTABN and mDTABN. In the ICT state of DTABN the amino group may very well be strongly twisted with respect to the phenyl ring. This conclusion is based on our observation that the ICT reaction of DTABN is ultrafast in *n*-hexane (70 fs) as well as in MeCN (60 fs). Large amplitude motions seem rather unlikely in such short times, leading to the conclusion that the amino twist angle θ in the ICT state will not deviate appreciably from that in its strongly twisted (75°) ground state. This condition of a strongly twisted ICT state may also hold for mDTABN, with $\theta = 86.5°$ in S_0, for which femtosecond ESA measurements have not been carried out. A similar argument based on the time needed for

large amplitude motions (the appearance of the ICT absorption from the planar ground state within 200 fs) was used as a support for our conclusion that the ICT state of DMABN is planar.[8]

A second argument for strongly twisted ICT states of DTABN and mDTABN comes from the observation of efficient ICT with mDTABN, whereas such a reaction is absent for all other meta-aminobenzonitriles investigated until now.[27−35] In such a strongly twisted ICT state, a substantial electronic decoupling of the di-*tert*-butylamino and the benzonitrile moieties will have taken place. This situation makes the DTABNs similar to other molecules with weakly interacting electron donor (D)/acceptor (A) parts, such as CBQ, for wich an efficient charge-transfer reaction occurs in the excited-state with the para- and meta-derivatives.[50]

We therefore conclude that the electronic coupling in the ICT state of DTABN and mDTABN is different from that in the planar ICT state of DMABN, being similar to that present with CBQ and the bianthryls 9,9′-bianthryl, 10-cyano-9,9′-bianthryl, and 10,10′-dicyano-9,9′-bianthryl. For these bianthryls, the ICT emission maximum shows a linear correlation with the redox potentials of the D and A subunits, which correlation is absent for dual fluorescing 4-aminobenzonitriles.[7,12,19,20]

Conclusions

From X-ray crystal analysis, it is found that the di(*tert*-butyl)-amino group of mDTABN in the ground state S_0 is strongly twisted with respect to the phenyl plane, with an amino twist angle θ of 86.5°. A similarly large angle θ of 75° is determined for DTABN from the absorption spectra of a series of aminobenzonitriles with known twist angles. Because of this pronounced amino twist, the amino group in DTABN and mDTABN has undergone a substantial electronic decoupling from the benzonitrile moiety. As a consequence, the extinction coefficient of the lowest-energy unstructured absorption bands of DTABN and mDTABN is relatively small (1120 and 620 M^{-1} cm^{-1}), around 25 times smaller than that of the planar DMABN (29370 M^{-1} cm^{-1}). The steric hindrance exerted by the two bulky di-*tert*-butylamino amino substituents in mDTABN results in exceptionally long amino−phenyl (143.7 pm) and amino−*tert*-butyl (150.4 pm) bonds. The corresponding lengths for DMABN are 136.5 and 144.8 pm.

From solvatochromic measurements, dipole moments of 17 D are determined from the fluorescence spectra of DTABN and mDTABN. These dipole moments are similar to those published for the ICT state of DMABN (17 D), DIABN (18 D), and NTC6 (19 D). The emission band of DTABN and mDTABN therefore originates from the ICT state. An LE fluorescence cannot be identified with certainty, its relative weakness being caused by the ultrafast LE → ICT reaction, with a shortest reaction time of 70 fs in *n*-hexane and 60 fs in MeCN at 22 °C.

The picosecond fluorescence decays of DTABN can be fitted with one decay time τ_1, increasing with solvent polarity from 0.86 ns in *n*-hexane to 3.48 ns in MeCN at 25 °C. This decay time is equal to the ICT lifetime τ'_0(ICT). The femtosecond ESA spectra of DTABN in *n*-hexane and MeCN at 22 °C resemble that of the ICT state of DMABN in MeCN, with some broadening from the absorption of the LE state. From the decay and simultaneous growing-in of the band integrals in the spectral ranges where either the LE or the ICT absorption dominates, an ICT reaction time of 70 fs (*n*-hexane) and 60 fs (MeCN) is determined for the pump−probe time interval 0.05−2.6 ps. The rise and decay times between 6.9 ps (*n*-hexane) and 12 ps (MeCN) obtained for the longer time interval (1−60 ps delay time) are ascribed to vibrational solvent cooling. The results indicate that the ICT state of DTABN and mDTABN is formed from the LE state as the precursor. From the starting condition with a strongly twisted amino group for DTABN (θ = 75°), and mDTABN (θ = 85.6°) in the ground state, together with the observation of an ultrafast LE → ICT reaction in *n*-hexane (70 fs) and MeCN (60 fs) at 22 °C, it is concluded that the amino group in the LE as well as the ICT state of DTABN and mDTABN is likewise strongly twisted. This conclusion is opposite to that made for DMABN and NTC6, examples for planar or weakly twisted aminobenzonitriles in S_0, for which an effectively planar LE and ICT state is assumed, i.e., a state with a substantial electronic coupling between the amino and benzonitrile moieties. Our finding that ICT not only occurs for the para-substituted DTABN, but also for its meta-derivative mDTABN, in contrast to what is the case with other aminobenzonitriles, is seen as a support for this conclusion. The observation of fast and efficient ICT with the meta-derivative mDTABN is unusual, as ICT has not previously been found with other 3-aminobenzonitrile such as mDMABN. This finding supports our conclusion that the amino group in the ICT state of DTABN and mDTABN is strongly twisted and hence decoupled, similar to that of CBQ.

Acknowledgment. Many thanks are due to Professor Nikolaus Ernsting, Humboldt University Berlin, for the use of the femtosecond absorption equipment in the investigations reported here. S.R.D. is very thankful to the Alexander von Humboldt Foundation for financial support. Many thanks are due to Mr. Jürgen Bienert for carrying out HPLC purifications and to Mr. Wilfried Bosch and Mr. Helmut Lesche for technical support. The interest of Dr. Silviu Balaban (Institute for Nanotechnology, Karlsruhe, Germany) in this subject is gratefully acknowledged.

Supporting Information Available: Text giving synthetic and experimental procedures for the preparation of DTABN and mDTABN and schemes showing the reactions used and a cif file for DTABN. This material is available free of charge via the Internet at http://pubs.acs.org.

References and Notes

(1) Lippert, E.; Lüder, W.; Boos, H. In *Advances in Molecular Spectroscopy; European Conference on Molecular Spectroscopy, Bologna, Italy, 1959*; Mangini, A., Ed.; Pergamon Press: Oxford, U.K., 1962; p 443.

(2) Lippert, E.; Lüder, W.; Moll, F.; Nägele, W.; Boos, H.; Prigge, H.; Seibold-Blankenstein, I. *Angew. Chem.* **1961**, *73*, 695.

(3) Grabowski, Z. R.; Rotkiewicz, K.; Rettig, W. *Chem. Rev.* **2003**, *103*, 3899.

(4) Rettig, W. *Angew. Chem., Int. Ed. Engl.* **1986**, *25*, 971.

(5) Leinhos, U.; Kühnle, W.; Zachariasse, K. A. *J. Phys. Chem.* **1991**, *95*, 2013.

(6) Okada, T.; Mataga, N.; Baumann, W. *J. Phys. Chem.* **1987**, *91*, 760.

(7) Zachariasse, K. A.; Grobys, M.; von der Haar, Th.; Hebecker, A.; Il'ichev, Yu. V.; Morawski, O.; Rückert, I.; Kühnle, W. *J. Photochem. Photobiol. A: Chem.* **1997**, *105*, 373.

(8) Druzhinin, S. I.; Ernsting, N. P.; Kovalenko, S. A.; Lustres, L. P.; Senyushkina, T. A.; Zachariasse, K. A. *J. Phys. Chem. A* **2006**, *110*, 2955.

(9) Su, S. G.; Simon, J. D. *J. Phys. Chem.* **1989**, *93*, 753.

(10) Kwok, W. M.; George, M. W.; Grills, D. C.; Ma, C.; Matousek, P.; Parker, A. W.; Phillips, D.; Toner, W. T.; Towrie, M. *Angew. Chem., Int. Ed.* **2003**, *42*, 1826.

(11) Schuddeboom, W.; Jonker, S. A.; Warman, J. M.; Leinhos, U.; Kühnle, W.; Zachariasse, K. A. *J. Phys. Chem.* **1992**, *96*, 10809.

(12) von der Haar, Th.; Hebecker, A.; Il'ichev, Yu. V.; Jiang, Y.-B.; Kühnle, W.; Zachariasse, K. A. *Recl. Trav. Chim. Pays-Bas* **1995**, *114*, 430.

(13) Zachariasse, K. A.; Grobys, M.; Tauer, E. *Chem. Phys. Lett.* **1997**, *274*, 372.

(14) Druzhinin, S. I.; Demeter, A.; Galievsky, V. A.; Yoshihara, T.; Zachariasse, K. A. *J. Phys. Chem. A* **2003**, *107*, 8075.

(15) Demeter, A.; Zachariasse, K. A. *Chem. Phys. Lett.* **2003**, *380*, 699.
(16) Howell, R.; Petek, H.; Phillips, D.; Yoshihara, K. *Chem. Phys. Lett.* **1991**, *183*, 249.
(17) Lommatzsch, U.; Gerlach, A.; Lahmann, Ch.; Brutschy, B. *J. Phys. Chem. A* **1998**, *102*, 6421.
(18) Daum, R.; Druzhinin, S. I.; Ernst, D.; Rupp, L.; Schroeder, J.; Zachariasse, K. A. *Chem. Phys. Lett.* **2001**, *341*, 272.
(19) Zachariasse, K. A.; Grobys, M.; von der Haar, Th.; Hebecker, A.; Il'ichev, Yu. V.; Jiang, Y.-B.; Morawski, O.; Kühnle, W. *J. Photochem. Photobiol. A: Chem.* **1996**, *102*, 59. Erratum: *J. Photochem. Photobiol. A: Chem.* **1998**, *115*, 259.
(20) Il'ichev, Yu. V.; Kühnle, W.; Zachariasse, K. A. *J. Phys. Chem. A* **1998**, *102*, 5670.
(21) Leinhos, U. Ph.D. Thesis, University of Göttingen, Göttingen, Germany 1991.
(22) Demeter, A.; Druzhinin, S.; George, M.; Haselbach, E.; Roulin, J.-L.; Zachariasse, K. A. *Chem. Phys. Lett.* **2000**, *323*, 351.
(23) Druzhinin, S. I.; Demeter, A.; Zachariasse, K. A. *Chem. Phys. Lett.* **2001**, *347*, 421.
(24) Zachariasse, K. A.; Druzhinin, S. I.; Bosch, W.; Machinek, R. *J. Am. Chem. Soc.* **2004**, *126*, 1705.
(25) Druzhinin, S. I.; Kovalenko, S. A.; Senyushkina, T.; Zachariasse, K. A. *J. Phys. Chem. A* **2007**, *111*, 12878.
(26) Visser, R. J.; Varma, C. A. G. O. *J. Chem. Soc. Faraday Trans. 2* **1980**, *76*, 453.
(27) Rettig, W.; Bliss, B.; Dirnberger, K. *Chem. Phys. Lett.* **1999**, *305*, 8.
(28) Oshima, J.; Shiobara, S.; Naoumi, H.; Kaneko, S.; Yoshihara, T.; Mishra, A. K.; Tobita, S. *J. Phys. Chem. A.* **2006**, *110*, 4629.
(29) Grabowski, Z. R.; Rotkiewicz, K.; Siemiarczuk, A.; Cowley, D. J.; Baumann, W. *Nouv. J. Chim.* **1979**, *3*, 443.
(30) Zachariasse, K. A.; von der Haar, Th.; Hebecker, A.; Leinhos, U.; Kühnle, W. *Pure Appl. Chem.* **1993**, *65*, 1745.
(31) Zachariasse, K. A. *Chem. Phys. Lett.* **2000**, *320*, 8.
(32) Jamorski Jödicke, Ch.; Lüthi, H.-P. *J. Chem. Phys.* **2003**, *119*, 12852.
(33) Findley, G. L.; Carsey, T. P.; McGlynn, S. P. *J. Am. Chem. Soc.* **1979**, *101*, 4511.
(34) Oshima, J.; Yoshihara, T.; Tobita, S. *Chem. Phys. Lett.* **2006**, *423*, 306.
(35) Parusel, A. B. J.; Schamschule, R.; Kohler, G. *Z. Phys. Chem.* **2002**, *216*, 361.
(36) Jamorski Jödicke, Ch.; Lüthi, H.-P. *J. Chem. Phys. Lett.* **2003**, *368*, 561.
(37) Yamamoto, H.; Maruoka, K. *J. Org. Chem.* **1980**, *45*, 2739.
(38) (a) Casarini, A.; Dembech, P.; Lazzari, D.; Marini, E.; Reginato, G.; Ricci, A.; Seconi, G. *J. Org. Chem.* **1993**, *58*, 5620. (b) Alberti, A.; Canè, F.; Dembech, P.; Lazzari, D.; Ricci, A.; Seconi, G. *J. Org. Chem.* **1996**, *61*, 1677.
(39) (a) del Amo, V.; Dubbaka, S. R.; Krasovskiy, A.; Knochel, P. *Angew. Chem., Int. Ed.* **2006**, *45*, 7838. (b) Kienle, M.; Dubbaka, S. R.; del Amo, V.; Knochel, P. *Synthesis*, **2007**, 1272.
(40) (a) Krasovskiy, A.; Knochel, P. *Angew. Chem., Int. Ed.* **2004**, *43*, 3333. (b) Krasovskiy, A.; Straub, B.; Knochel, P. *Angew. Chem., Int. Ed.* **2006**, *45*, 159.
(41) Yoshihara, T.; Druzhinin. S. I.; Demeter, A.; Kocher, N.; Stalke, D.; Zachariasse, K. A. *J. Phys. Chem. A* **2005**, *109*, 1497.
(42) Galievsky, V. A.; Druzhinin, S. I.; Demeter, A; Jiang, Y.-B.; Kovalenko, S. A.; Lustres, L. P.; Venugopal, K.; Ernsting, N. P.; Allonas, X.; Noltemeyer, M.; Machinek, R.; Zachariasse, K. A. *Chem. Phys. Chem.* **2005**, *6*, 2307.
(43) Kovalenko, S. A.; Dobryakov, A. L.; Ruthmann, J.; Ernsting, N. P. *Phys. Rev. A* **1999**, *59*, 2369.
(44) Ernsting, N. P.; Kovalenko, S. A.; Senyushkina, T. A.; Saam, J.; Farztdinov, V. *J. Phys. Chem. A* **2001**, *105*, 3443.
(45) Altomare, A.; Burla, M. C.; Camalli, M.; Cascarano, G. L.; Giacovazzo, C.; Guagliardi, A.; Moliterni, A. G. G.; Polidori, G.; Spagna, R. *J. Appl. Crystallogr.* **1999**, *32*, 115.
(46) Sheldrick, G. M. *SHELXS-97 and SHELXL-97, Programs for the Solution and Refinement of Crystal Structures*; University of Göttingen: Göttingen, Germany, 1997.
(47) Druzhinin, S. I.; Dix, I.; Mayer, P.; Noltemeyer, M.; Zachariasse, K. A. Manuscript in preparation.
(48) Heine, A.; Herbst-Irmer, R.; Stalke, D.; Kühnle, W.; Zachariasse, K. A. *Acta Crystallogr.* **1994**, *B50*, 363.
(49) Techert, S.; Zachariasse, K. A. *J. Am. Chem. Soc.* **2004**, *126*, 5593.
(50) Druzhinin, S. I.; Galievsky, V. A.; Kovalenko, S. A.; Noltemeyer, M.; Zachariasse, K. A. Manuscript in preparation.
(51) March, J. *Advanced Organic Chemistry*, 4th ed.; Wiley: New York, 1992; p 21.
(52) Exner, O.; Vetešník, P. *Collect. Czech. Chem. Commun.* **1980**, *70*, 444.
(53) Rotkiewicz, K.; Rubaszewska, W. *Chem. Phys. Lett.* **1978**, *43*, 2763.
(54) Köhler, G.; Rechthaler, K.; Grabner, G.; Luboradzki, R.; Suwińska, K.; Rotkiewicz, K. *J. Phys. Chem. A* **1997**, *101*, 8518.
(55) Bulliard, C.; Allan, M.; Wirtz, G.; Haselbach, E.; Zachariasse, K. A.; Detzer, N.; Grimme, S. *J. Phys. Chem. A* **1999**, *103*, 7766.
(56) Carsey, T. P.; Findley, G. L.; McGlynn, S. P. *J. Am. Chem. Soc.* **1979**, *101*, 4502.
(57) Burgers, J.; Hoefnagel, M. A.; Verkade, P. E.; Visser, H.; Wepster, B. M. *Recl. Trav. Chim. Pays-Bas* **1958**, *77*, 491.
(58) Rückert, I.; Hebecker, A.; Parusel, A. B. J.; Zachariasse, K. A. *Z. Phys. Chem.* **2000**, *214*, 1597.
(59) From a quadratic fit of $\cos^2\theta$, where θ is the amino twist angle, against the extinction coefficient ϵ^{max} of the maximum of the lowest-energy absorption band for the molecules in Table 4, a value of $\theta = 75.2°$ is obtained for DTABN. A linear fit of $\cos^2\theta$ vs ϵ^{max} leads to a similar value: $\theta = 75.9°$.
(60) Yoshihara, T.; Galievsky, V.; Druzhinin, S. I.; Saha, S.; Zachariasse, K. A. *Photochem. Photobiol. Sci.* **2003**, *2*, 342.
(61) Decay times τ_i are numerated starting with τ_1 as the longest time. In the present case of DTABN, τ_1 is the nanosecond ICT lifetime τ'_0(ICT) (Table 7), τ_2 is the solvent cooling time (2−12 ps, Table 8) and τ_3 is the ICT reaction time of 70 fs in *n*-hexane and 60 fs in MeCN (Table 8).
(62) Schwarzer, D.; Troe, J.; Zerezke, M. *J. Chem. Phys.* **1997**, *107*, 8380.